Supporting Information of

Solid state molecular motions in Cd-based halides monitored by photoluminescence switching

Jie-Ru Yang,[†a] Yingchen Peng,[†b] Huai-Yu Wu,[a] Si-Yu Xu,[a] Jiawei Lin,[a] Xuexia Lu,[a] Chuanhua Wu,[a] Miao-Bin Xu[a], Xinghui Qi,[c*] Ye Yang,[b*] Jin Chen,[a*] Xiao-Ying Huang,[d] Ke-Zhao Du[a*]

[a]*College of Chemistry and Materials Science, Fujian Key Laboratory of polymer Materials, Fujian Normal University, Fuzhou 350007, China.*

[b]*State Key Laboratory of Physical Chemistry of Solid Surfaces, College of Chemistry and Chemical Engineering, Xiamen University, Xiamen 361005, China*

[c]*The International Joint Institute of Tianjin University, Fuzhou, Tianjin University, Tianjin 300072, China*

[d]*State Key Laboratory of Structural Chemistry, Fujian Institute of Research on the Structure of Matter, Chinese Academy of Sciences, Fuzhou 350002, China.*

†These authors contributed equally

E-mail addresses: xhqi@tjufz.org.cn; cj2015@fjnu.edu.cn (J.C.); ye.yang@xmu.edu.cn (Y.Y); duke@fjnu.edu.cn (K.-Z. Du.);

MATERIALS AND METHODS

Materials and synthesis

CdO (>99%), piperazine (>99%), HI (55–58% wt), HCl (37% wt), HBr(48% wt) were used as purchased from Adamas-beta.

The synthesis conditions for **Cd-I**, **CdI-P**, **Cd-ICl**, **Cd-IBr** and (PIP)CdI$_4$·PIP·2I, yielding larger crystals and higher yields, are outlined as follows:

*Synthesis of (PIP)CdI$_4$ (namely, **Cd-I**)*: CdO (256.8 mg, 2 mmol), piperazine (86.14 mg, 1 mmol), HI (2 mL), and H$_2$O (1 mL) were sealed in Teflon pouches (25 mL) and placed in an autoclave. The autoclave was heated to 90 °C for 72 hours and then cooled to 30 °C at a rate of 1.67 °C/h. Yellow block-shaped crystals of **Cd-I** were obtained with high yields of approximately 95% (based on Cd).

*Synthesis of (PIP)CdI$_4$···PIP·2Cl (namely, **CdI-P**):* CdO (25.68 mg, 0.2 mmol), piperazine (86.14 mg, 1 mmol), HI (1 mL), HCl (1 mL), and H$_2$O (1 mL) were used as starting materials. Similar to the procedure for **Cd-I**, the mixture was sealed in Teflon pouches (25 mL) and heated at 110 °C for 72 hours, followed by cooling to 30°C at a rate of 1.67 °C/h. Yellow block-shaped crystals of **CdI-P** were obtained with high yields of approximately 80% (based on Cd).

*Synthesis of (PIP)CdI$_2$Cl$_2$ (namely, **Cd-ICl**)*: CdO (256.8 mg, 2 mmol), piperazine (86.14 mg, 1 mmol), HI (1 mL), HCl (1 mL), and H$_2$O (1 mL) as starting materials. The synthesis process was similar to that of compounds **Cd-I** and **CdI-P**, with heating at 110 °C for 72 hours and subsequent cooling to 30 °C at a rate of 1.67 °C/h. Yellow block-shaped crystals of **Cd-ICl** were obtained with high yields of approximately 95% (based on Cd).

*Synthesis of (PIP)CdI$_{2.4}$Br$_{1.6}$ (namely, **Cd-IBr**)*: CdO (256.8 mg, 2 mmol), piperazine (86.14 mg, 1 mmol), HI (1 mL), HBr (1 mL), and H$_2$O (1 mL) were employed as starting materials. The synthesis procedure resembled that of **Cd-I**, **CdI-P** and **Cd-ICl**, with heating at 110 °C for 72 hours and cooling to 30 °C at a rate of 1.67 °C/h. Yellow block-shaped crystals of **Cd-IBr** were obtained with high yields of approximately 95% (based on Cd).

Synthesis of (PIP)CdI$_4$·PIP·2I: **Cd-I** (708.16 mg, 1 mmol) and PIP·2I (342.14 mg, 1 mmol) were ground into powder and recrystallized with water to form colorless block crystals.

Characterization methods

Single Crystal Structure Determination

Single-crystal X-ray diffraction data for the title compounds were collected using two different diffractometers: an Xcalibur Eos Gemini diffractometer with Mo Kα radiation (λ = 0.71073 Å) at 293 K, and a Rigaku XtaLAB Synergy-DW dual-wavelength CCD diffractometer with Cu Kα radiation (λ = 1.54184 Å) at 109 K. Data reduction was performed using CrysAlisPro, and absorption correction based on the multi-scan method was applied. The structures of **Cd-I**, **CdI-P**, **Cd-ICl**, **Cd-IBr** and (PIP)CdI$_4$·PIP·2I were determined using direct methods and refined by full-

matrix least-squares fitting on F^2 using SHELXL-2014[1]. All non-hydrogen atoms were refined with anisotropic thermal parameters. The structure was checked for missing symmetry elements using PLATON, and none were found[2]. Crystallographic data and structural refinements of **Cd-I**, **CdI-P**, **Cd-ICl**, **Cd-IBr** and (PIP)CdI$_4$·PIP·2I have been listed in Tables S1

Powder X-ray Diffraction (PXRD).

The PXRD analysis was conducted using a Rigaku Ultima IV diffractometer, utilizing copper Kα radiation. Operating parameters were set to 40 kV for voltage and 40 mA for current. The diffraction data were gathered within the angular range of 5° to 65°, employing a step size of 10° per minute. Additionally, a theoretical powder X-ray diffraction pattern was generated based on the single-crystal structure.

Thermogravimetry Analysis (TGA).

TGA was performed on a Rigaku TG-DTA 8121 unit under an Ar atmosphere in the temperature range 30-800 °C at a rate of 10 °C min^{-1} in an argon flux (40 mL min^{-1}).

Absorption Spectrum Measurements.

The ultraviolet-visible-infrared (UV-vis-IR) spectrum in the range of 200-800 nm was recorded using a PerkinElmer Lambda 750 UV-vis-NIR spectrophotometer. The reflectance spectrum was transformed into an absorption spectrum using the Kubelka–Munk function[3].

Infrared Spectrum Test

The infrared (IR) spectrum was recorded on a Thermo Fisher Nicolet 5700 FT-IR spectrometer in the form of KBr pellets in the range from 4000 to 400 nm^{-1}.

Photoluminescence Property Characterization.

The PL properties including excitation and emission spectra as well as photoluminescence quantum yield (PLQY) were collected on an EDINBURGH FS 5 fluorescence spectrometer equipped with an integrating sphere. The calculation of PLQY is based on the equation of $\eta_{QE} = I_S/(E_R - E_S)$, where I_S is the luminescence emission intensity of sample, E_R and E_S represent the excitation spectra from the empty integrated sphere and sample, respectively.

Femtosecond Transient Absorption

The femtosecond transient absorption (fs-TA) spectroscopy setup is powered by a Ti: sapphire laser amplifier (Coherent Astrella-Tunalbe-USP, USA), which can generate 800 nm pulse train with a temporal pulse width of 35 fs, pulse energy of 6.1 mJ and repetition frequency of 1000 Hz. The fundamental beam was spited into two branches. A branch of the fundamental beam was attenuated

and focused into a sapphire crystal to generate the broadband probe pulses in the visible regions (450-800 nm). The pump pulses of 257 and 400 nm were generated by two ways. A part of the fundamental beam was introduced into an optical parametric amplifier (OPA) to generate monochrome pulses with different wavelength. The frequency of 515 nm monochrome beam was doubled into 257 nm pump pulse by an BBO crystal (HG OPTRONICS., INC.). The frequency of another branch of another fundamental beam was doubled into 400 nm by another BBO crystal (HG OPTRONICS., INC.). The pump pulses (257 or 400 nm) were then chopped at the frequency of 500 Hz by an optical chopper. The pump pulse energy was attenuated by neutral density filter wheels. The time delay between pump and probe pulses was controlled by a motorized translation stage. The pump and probe pulses were focused on the same spot of the single crystal sample. The focal size of the pump was adjusted intentionally to be much greater than that of the probe so that the excitation density in the probing area was homogenous. The transmitted probe pulses were then sent into to the visible spectrometers. The sample was stable, and no precipitate was appeared during the experiment. Spectrum or kinetics changes due to photodegradation was not observed based on scan to scan comparisons.

Density functional theory

The electronic structures of compounds were computed using the plane-wave pseudopotential method within the framework of density functional theory (DFT), as implemented in the total energy code Cambridge Sequential Total Energy Package (CASTEP)[4, 5]. For the exchange-correlation functional, we selected the Perdew-Burke-Ernzerhof (PBE) formula within the generalized gradient approximation (GGA)[6].

Table S1. Crystallographic data for **Cd-I**, **CdI-P**, **Cd-ICl**, **Cd-IBr** and (PIP)CdI$_4$·PIP·2I.

Compound	Cd-I	CdI-P	Cd-ICl	Cd-IBr	(PIP)CdI$_4$·PIP·2I
CCDC Number	175861	2381801	2381800	2381799	2404363
Empirical formula	C$_4$H$_{12}$CdI$_4$N$_2$	C$_8$H$_{24}$CdCl$_2$I$_4$N$_4$	C$_4$H$_{12}$CdCl$_2$I$_2$N$_2$	C$_4$H$_{12}$Br$_{1.6}$CdI$_{2.4}$N$_2$	C$_8$H$_{24}$CdI$_6$N$_4$
Formula weight	708.16	867.21	525.26	634.38	1050.11
Temperature/K	293(2)	274.1(3)	293(2)	273.15(12)	293(2)
Crystal system	orthorhombic	monoclinic	monoclinic	orthorhombic	monoclinic
Space group	$P2_12_12_1$	$C2/c$	$C2/c$	$P2_12_12_1$	$C2/c$
a/Å	9.0318(5)	10.13180(10)	11.3343(2)	8.8562(2)	10.2216(2)
b/Å	12.2358(6)	9.4889(2)	12.0155(2)	12.0536(2)	9.7456(2)
c/Å	13.0518(7)	21.8916(2)	10.0864(2)	12.7689(3)	23.3106(4)
β/°	90	93.7510(10)	110.087(2)	90	93.911(2)
V/Å^3	1442.37(13)	2100.14(5)	1290.08(4)	1363.07(5)	2316.69(8)
Z	4	4	4	4	4
ρ_{calc}g/cm^3	3.261	2.743	2.704	3.091	3.011
μ/mm^{-1}	10.037	56.797	54.599	61.109	70.295
F(000)	1240.0	1576.0	952.0	1127.0	1864.0
Crystal size/mm^3	0.1×0.1×0.1	0.2×0.2×0.2	0.2×0.2×0.2	0.2×0.2×0.1	0.1×0.1×0.1
Radiation	Mo Kα (λ = 0.71073)	Cu Kα (λ = 1.54184)	Cu Kα (λ = 1.54184)	Cu Kα (λ = 1.54184)	Cu Kα (λ = 1.54184)
2θ range for date collection/°	7.076 to 52.742	8.094 to 154.914	11.104 to 156.236	10.092 to 156.09	7.602 to 153.584
Index ranges	-10 ≤ h ≤ 11, -14 ≤ k ≤ 15, -16 ≤ l ≤ 15	-12 ≤ h ≤ 12, -11 ≤ k ≤ 11, -22 ≤ l ≤ 27	-14 ≤ h ≤ 14, -15 ≤ k ≤ 13, -12 ≤ l ≤ 12	-11 ≤ h ≤ 6, -15 ≤ k ≤ 14, -16 ≤ l ≤ 16	-12≤h≤12, -12≤k≤9, -29≤l≤27
Reflections collected	10982	10977	9382	7716	11571
Independent refls	2902 [R$_{int}$ = 0.0641, R$_{sigma}$ = 0.0577]	2190 [R$_{int}$ = 0.0614, R$_{sigma}$ = 0.0314]	1384 [R$_{int}$ = 0.0393, R$_{sigma}$ = 0.0217]	2695 [R$_{int}$ = 0.0686, R$_{sigma}$ = 0.0568]	2372 [R$_{int}$ = 0.0633, R$_{sigma}$ = 0.0456]
GOF	1.047	1.077	1.061	1.052	1.037
R_1, wR_2 [I >2$\sigma(I)$]$_a$	R_1 = 0.0408, wR_2 = 0.0850	R_1 = 0.0422, wR_2 = 0.1132	R_1 = 0.0325, wR_2 = 0.0813	R_1 = 0.0509, wR_2 = 0.1306	R$_1$ = 0.0443, wR$_2$ = 0.1201
R_1, wR_2 (all data)a	R_1 = 0.0461, wR_2 = 0.0883	R_1 = 0.0434, wR_2 = 0.1146	R_1 = 0.0342, wR_2 = 0.0825	R_1 = 0.0535, wR_2 = 0.1324	R$_1$ = 0.0492, wR$_2$ = 0.1237
Largest diff. peak/hole / e Å^{-3}	1.26/-1.20	2.05/-1.55	1.19/-1.21	1.76/-2.00	1.62/-1.75

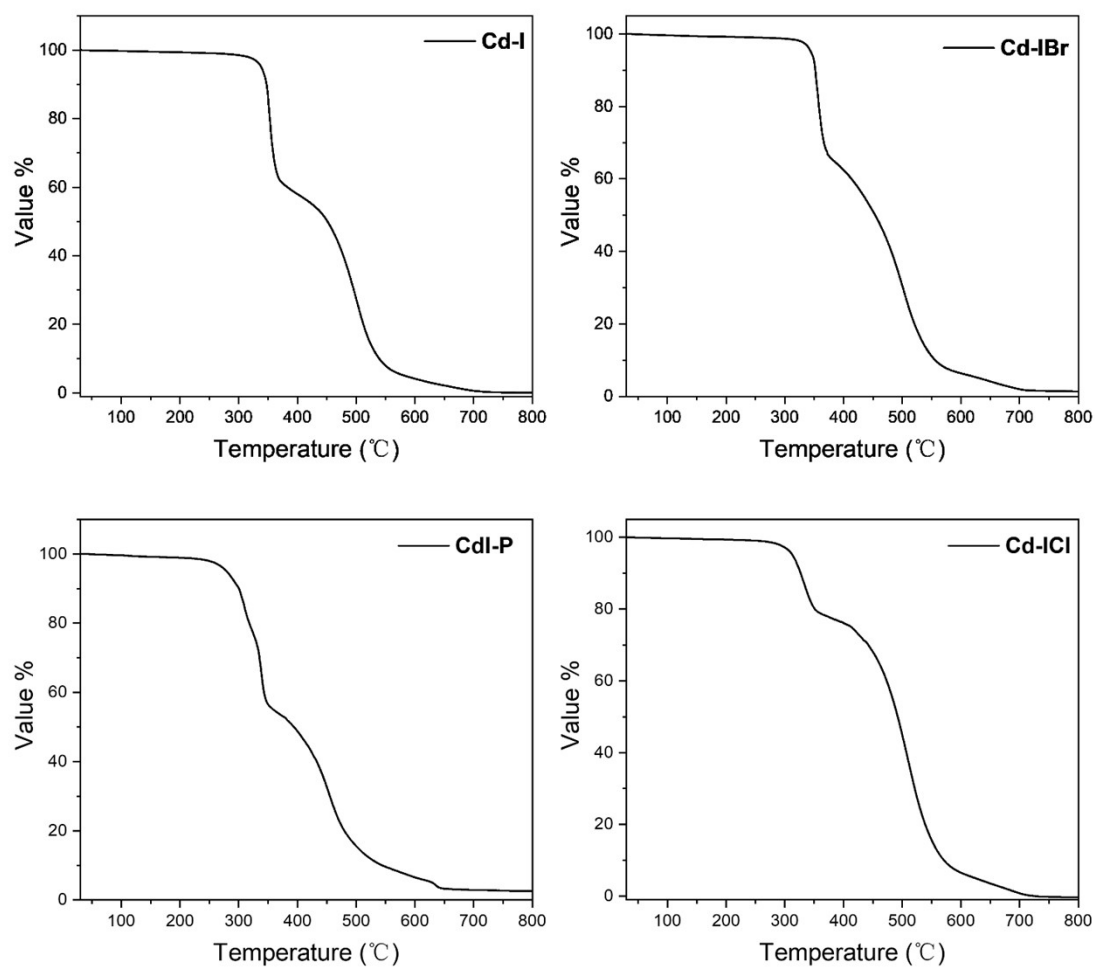[a]$R_1 = \sum||F_o| - |F_c||/\sum|F_o|$, and $wR_2 = \{\sum w[(F_o)^2 - (F_c)^2]^2/\sum w[(F_o)^2]^2\}^{1/2}$.

Figure S1. TGA spectra of **Cd-I**, **Cd-ICl**, **Cd-IBr** and **CdI-P**.
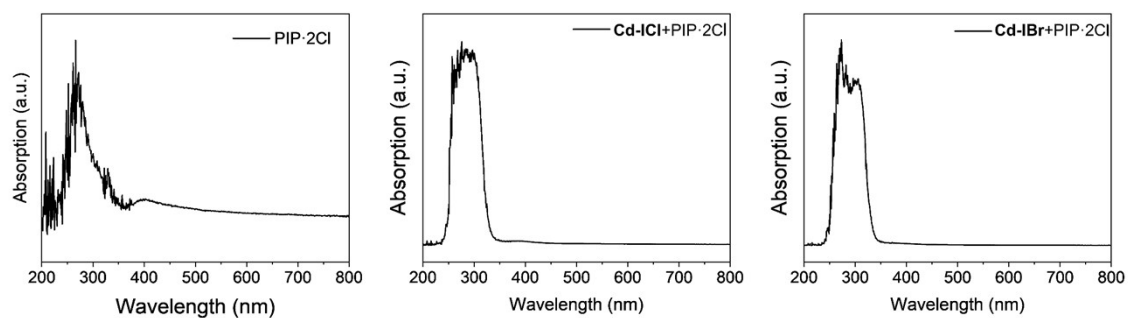

Figure S2. Absorption spectrum of PIP·2Cl, **Cd-ICl**+ PIP·2Cl and **Cd-IBr**+ PIP·2Cl.
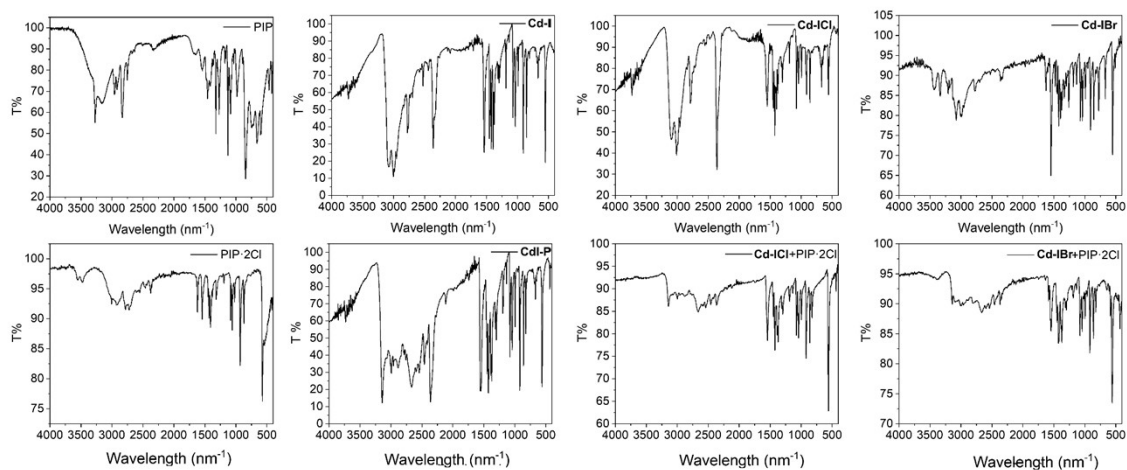
Figure S3. IR spectra of PIP, PIP·2Cl, **Cd-I**, **Cd-ICl**, **Cd-IBr**, **CdI-P**, **Cd-ICl+** PIP·2Cl and **Cd-IBr+** PIP·2Cl.
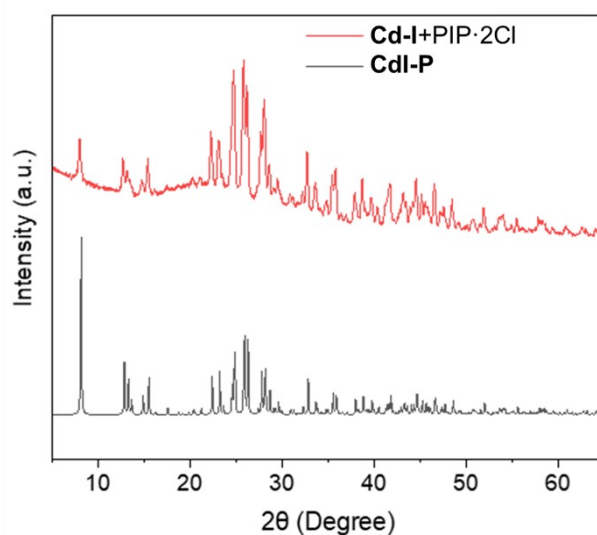

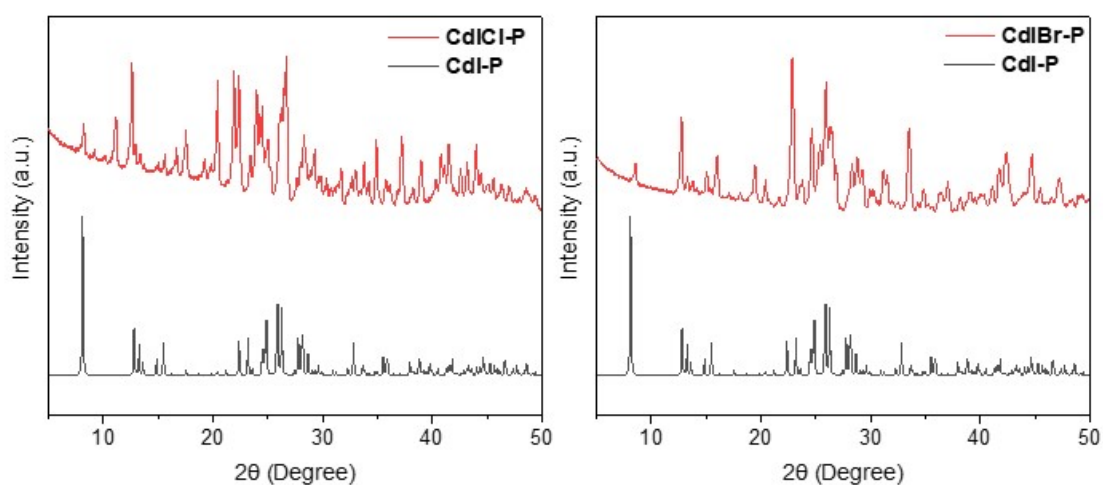**Figure S4.** Experimental and simulated PXRD comparison of **Cd-I** ground with PIP·2Cl, and **CdI-P**.

Figure S5. Experimental of **Cd-IBr** (left) and **Cd-ICl** (right) ground with PIP·2Cl compared with

the simulated PXRD of **CdI-P**.
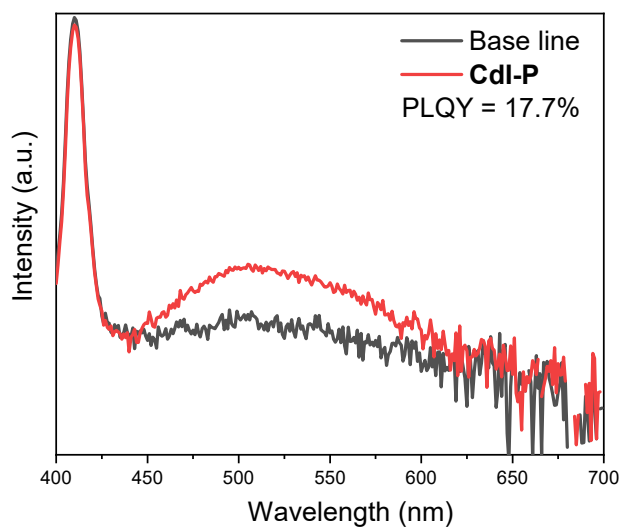
Figure S6. PLQY of **CdI-P**.

Figure S7. The transformation of **Cd-I** into the luminescent phases (PIP)CdI$_4$·PIP·2I under visible light (left) and UV light (right).
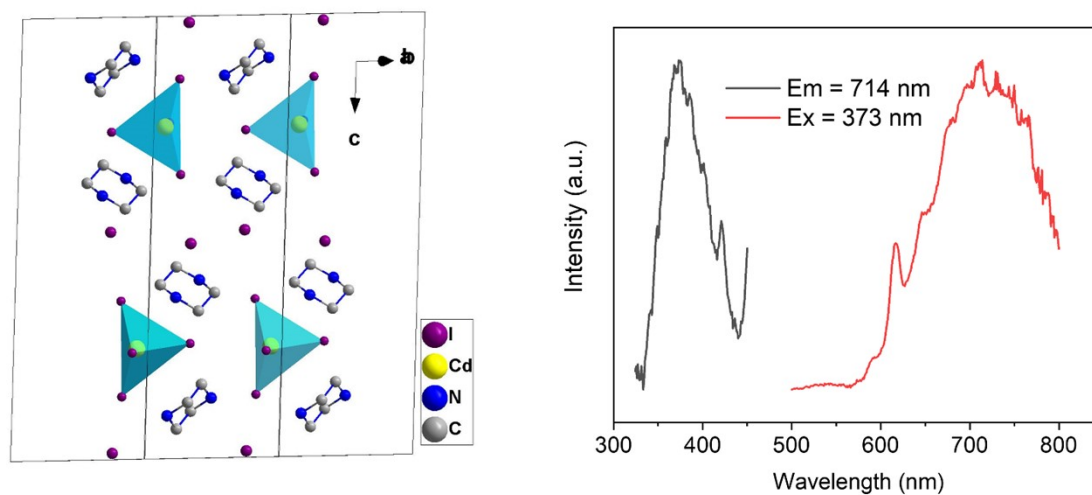
Figure S8. Structure of (PIP)CdI$_4$·PIP·2I (left), and photoluminescence excitation (PLE) and photoluminescence (PL) spectra of (PIP)CdI$_4$·PIP·2I (right).
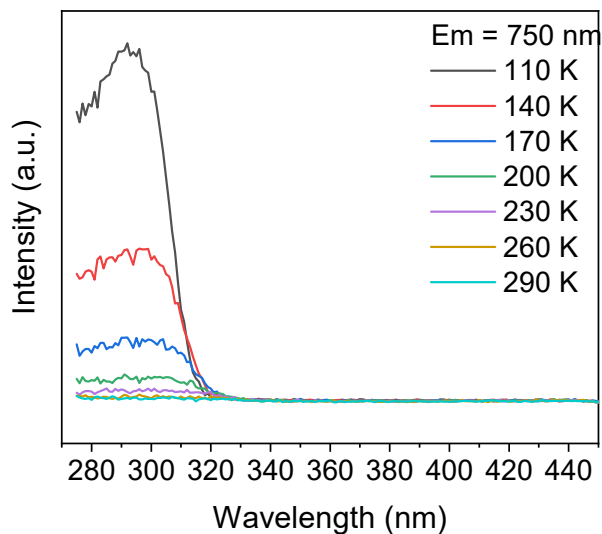
Figure S9. PLE spectra of crystal **CdI-P** at 80 K, 110 K, 140 K, 170 K, 200 K, 230 K, 260 K, and 290 K under emission wavelengths of 750 nm
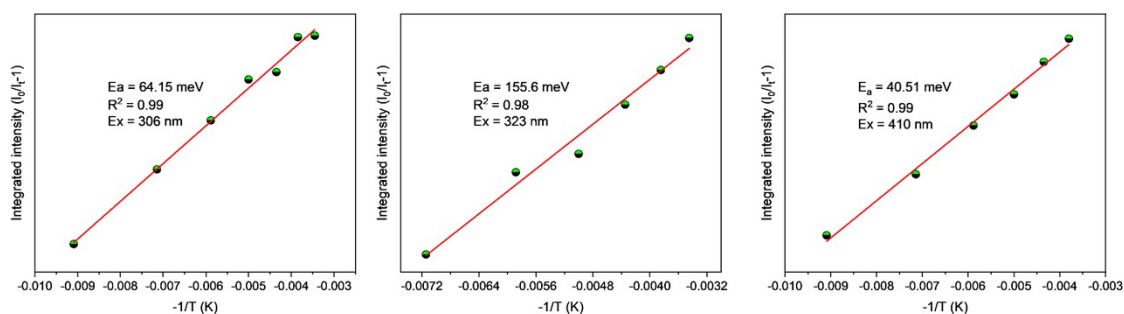

Figure S10. Temperature-dependent PL intensity variation for **CdI-P**. The laser excitation wavelength is 306 nm, 410 nm, 323 nm.
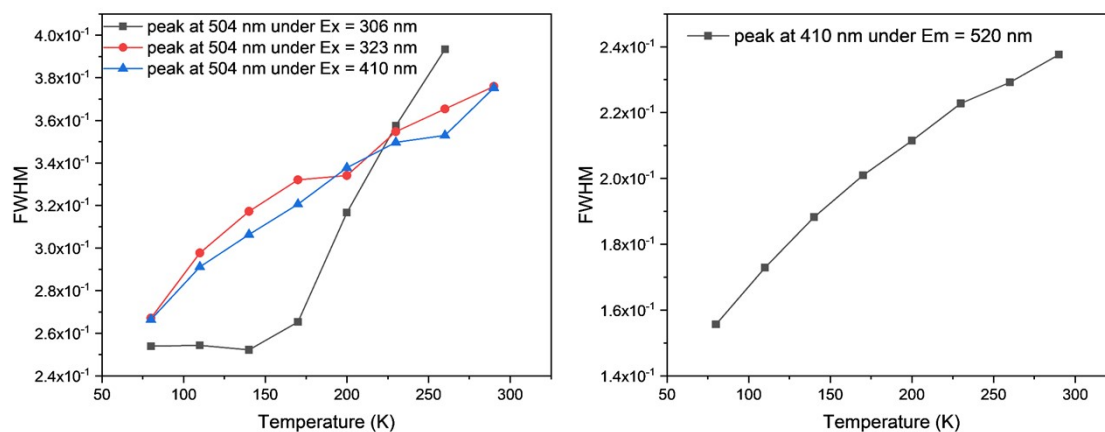

Figure S11. Temperature-dependent FWHM of PL and PLE for **CdI-P** at Ex = 306 nm, Ex = 323 nm, Ex = 410 nm and Em = 520 nm.
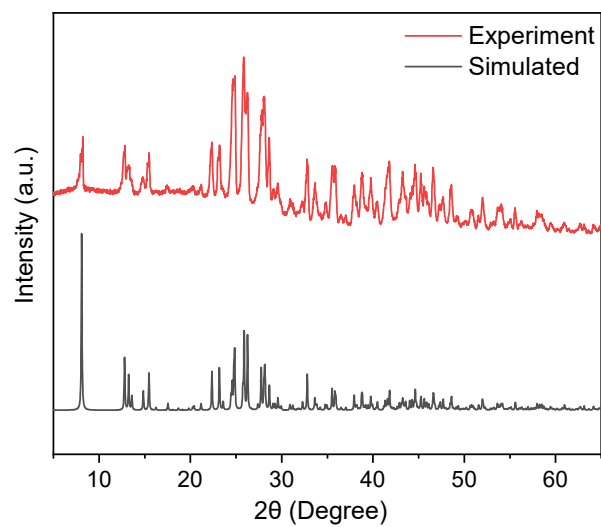
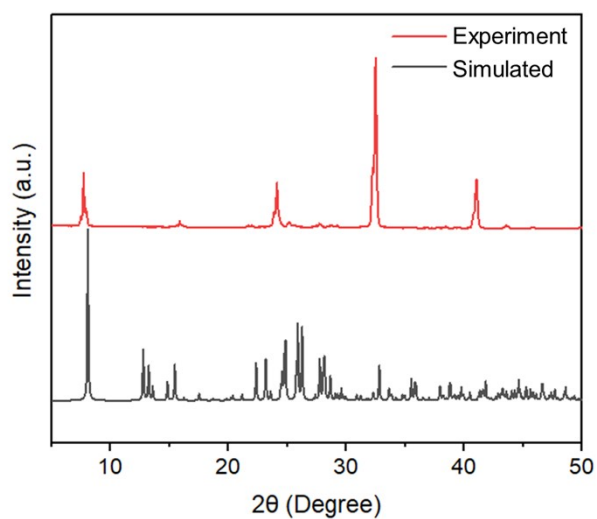**Figure S12.** The PXRD of **CdI-P** after two months exposure to air

Figure S13. Comparison of recrystallization PXRD with the original PXRD for **CdI-P**.
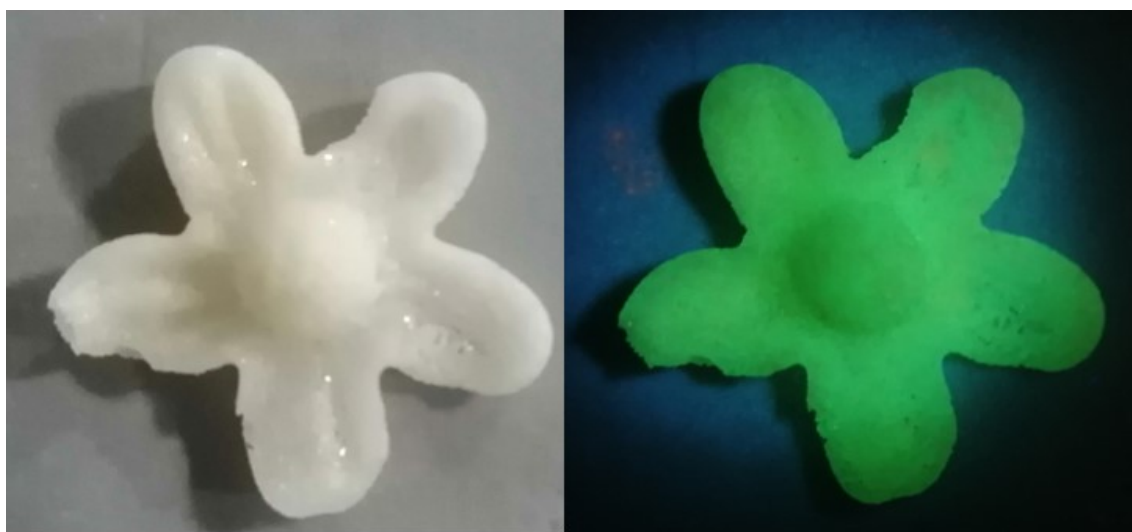
Figure S14. CdI-P pattern processed through solution method, under natural light (left) and UV light (right).

References

1. G.M. Sheldrick, Crystal structure refinement with SHELXL. *Acta Crystallogr C Struct Chem* **2015,** *71* (Pt 1), 3-8.

2. A.L. Spek, Single-crystal structure validation with the program . *J Appl Crystallogr* **2003,** (36), 7-13.

3. P. Kubelka; Munk, F., An Article on Optics of Paint Layers. *Z. Tech. Phys* **1931,** *12*, 259-274.

4. B.R.H. BLESSING, An Empirical Correction for Absorption Anisotropy. *Acta Crystallogr A* **1995,** *51*, 33-38.

5. B.W. V. MILMAN, J. A. WHITE, C. J. PICKARD, M. C. PAYNE, E. V. AKHMATSKAYA, R. H. NOBES, Electronic Structure, Properties, and Phase Stability of Inorganic Crystals: A Pseudopotential Plane-Wave Study. *Int J Quantum Chem* **1999,** *77*, 895–910.

6. P.J.D.L. M D Segall, MJProbert, C J Pickard,PJ Hasnip, S J Clark andMCPayne, First-principles simulation: ideas, illustrations and the CASTEP code. *Journal of physics: condensed matter* **2002,** *14*, 2717–2744.